Surface Functionalization of Thin-Film Composite Membranes with Copper Nanoparticles for Antimicrobial Surface Properties

ARTICLE *in* ENVIRONMENTAL SCIENCE & TECHNOLOGY · DECEMBER 2013

Impact Factor: 5.33 · DOI: 10.1021/es404232s · Source: PubMed

6 AUTHORS, INCLUDING:

Katherine R Zodrow
Yale University
17 PUBLICATIONS **609** CITATIONS
SEE PROFILE

Emmanuel Giannelis
Cornell University
312 PUBLICATIONS **20,752** CITATIONS
SEE PROFILE

Menachem Elimelech
Yale University
394 PUBLICATIONS **32,588** CITATIONS
SEE PROFILE

Environmental Science & Technology

Article

pubs.acs.org/est

Surface Functionalization of Thin-Film Composite Membranes with Copper Nanoparticles for Antimicrobial Surface Properties

Moshe Ben-Sasson,[†] Katherine R. Zodrow,[†] Qi Genggeng,[‡] Yan Kang,[‡] Emmanuel P. Giannelis,[‡] and Menachem Elimelech*,[†]

[†]Department of Chemical and Environmental Engineering Yale University New Haven, Connecticut 06520-8286, United States

[‡]Department of Materials Science and Engineering Cornell University Ithaca, New York 14853, United States

Supporting Information

ABSTRACT: Biofouling is a major operational challenge in reverse osmosis (RO) desalination, motivating a search for improved biofouling control strategies. Copper, long known for its antibacterial activity and relatively low cost, is an attractive potential biocidal agent. In this paper, we present a method for loading copper nanoparticles (Cu-NPs) on the surface of a thin-film composite (TFC) polyamide RO membrane. Cu-NPs were synthesized using polyethyleneimine (PEI) as a capping agent, resulting in particles with an average radius of 34 nm and a copper content between 39 and 49 wt.%. The positive charge of the Cu-NPs imparted by the PEI allowed a simple electrostatic functionalization of the negatively charged RO membrane. We confirmed functionalization and irreversible binding of the Cu-NPs to the membrane surface with SEM and XPS after exposing the membrane to bath sonication. We also demonstrated that Cu-NP functionalization can be repeated after the Cu-NPs dissolve from the membrane surface. The Cu-NP functionalization had minimal impact on the intrinsic membrane transport parameters. Surface hydrophilicity and surface roughness were also maintained, and the membrane surface charge became positive after functionalization. The functionalized membrane exhibited significant antibacterial activity, leading to an 80−95% reduction in the number of attached live bacteria for three different model bacterial strains. Challenges associated with this functionalization method and its implementation in RO desalination are discussed.

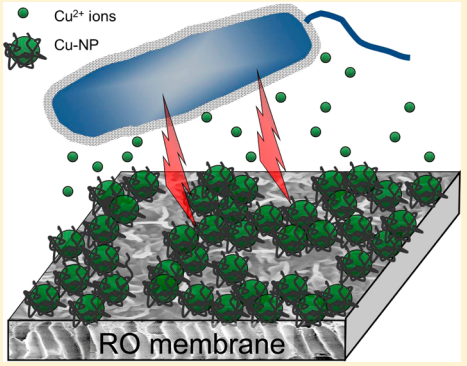

INTRODUCTION

As the world population continues to grow and increase demand for water resources, the supply of water in arid and semiarid regions will rely more on desalinated water.[1] In the past two decades, several seawater and brackish water reverse osmosis (RO) desalination plants have been constructed worldwide. Still, engineering challenges continue to limit development of additional plants and increase energy demand, chemical use, and operational costs of existing ones.

Biofouling is one of the most challenging problems in membrane desalination processes.[2,3] The difficulties in biofilm prevention and control arise from the ability of bacteria to thrive and create cohesive biofilm structures even under extreme conditions.[2,4,5] In RO desalination, biofouling poses a unique challenge because the predominantly used membrane in RO plants, thin-film composite (TFC) polyamide, cannot tolerate oxidants, such as the commonly used and relatively inexpensive chlorine[6] or its derivatives.[7] Therefore, alternative biofouling mitigation strategies need to be developed.

Strategies for improving RO membrane resistance to biofouling include grafting polymers[8−10] or nanoparticles (NPs)[11] to the membrane surface to modify surface properties, making it resistant to the adhesion of natural organic matter (NOM), proteins, and bacteria. Another biofouling control strategy involves anchoring biocidal polymers[12−14] or biocidal NPs[15] to the membrane surface. This particular strategy utilizes contact-killing, where bacteria are inactivated upon contact with the toxic polymers or NPs on the membrane surface. However, while the above two strategies mitigate biofouling in the short run, they do not eliminate fouling in the long run.[16] Over time, the RO membrane surface will likely be covered by the foulants in the feedwater that were able to pass through the pretreatment stages. Because the active NPs or polymers used in these biofouling control strategies act through contact with the bacteria, the deposited fouling layer significantly weakens their biofouling resistance activity.[16]

In an alternative biofouling control strategy, NPs that act as a source of biocides are bound to the membrane surface,[17] continually releasing biocides into the boundary layer above the membrane to form an inhibition zone.[18] Although a fouling layer on the membrane may change the biocide release dynamics, it will not prevent diffusion of the released biocidal species from the membrane surface through the foulant layer into the inhibition zone. Because of their small size, NPs can bind to the membrane surface with minimal effects on the RO

Received: September 23, 2013
Revised: December 3, 2013
Accepted: December 5, 2013
Published: December 5, 2013

module hydrodynamics, and thus, they are an attractive source for biocide release.

In several recent studies, antibacterial properties have been imparted to microfiltration (MF)[19] or ultrafiltration (UF)[17,20−22] membranes by embedding or binding biocide sources, including silver NPs. However, because biocides pass through the large pores of MF and UF membranes, the released biocidal species will be lost to the permeate, and only a low concentration of the biocide will be available at the membrane surface. Therefore, these types of surface modifications have a relatively short and low antibacterial effect in MF and UF. Additionally, the biocides will enter into the product water, potentially causing an environmental or health hazard.

Several advantages exist in using NPs as a biocide release source in salt-rejecting membrane processes, such as RO. In RO, the biocide is rejected by the selective barrier of the membrane, thereby lowering the risk of biocide permeation into the product water. Moreover, due to concentration polarization, the retained biocides will concentrate at the membrane surface, making the biocide available in the vicinity of the membrane surface, where the biofilm grows. Still, the depletion of the biocide source on the membrane will require frequent recharging for long-term operation. Therefore, it is not only sufficient to load the biocide source on the membrane, but it is also critical to demonstrate the ability to recharge the source after its depletion. Frequent recharging of the biocide source will also require consideration of biocide cost and the consequences of biocide presence in the RO concentrate (brine).

Silver-containing nanoparticles (Ag-NPs) are one of the most researched sources of biocide release for combating biofouling in TFC membrane processes, including RO.[23,24] However, while silver is a highly effective biocide, it is relatively expensive,[25] motivating a search for more economical yet effective biocides. Copper is one such alternative, having a long history (>2400 years) as an effective biocide,[26] and both copper ions and nanoparticles (Cu-NPs) have demonstrated antibacterial activity against numerous bacterial strains.[27−31] Copper continues to be used today in many biofouling control applications,[27,32,33] and it is included as a leachable biocidal agent in marine paints to control biofouling on ship hulls.[34] Notably, copper is relatively inexpensive, with a cost of approximately 1% that of silver.[25]

To date, few studies have incorporated copper in membrane separation processes for biofouling control, targeting UF membranes.[35−37] However, while an antibacterial effect was reported, it was not clear how the ions or imbedded NPs interacted with the bacteria. Copper-sulfate salt was demonstrated as an effective biocide to improve RO membrane cleaning efficiency,[38] and coating RO spacers with copper imparted antibacterial activity to the membrane module.[39,40] To date, mitigating biofouling by functionalization of the TFC membrane surface with Cu-NPs that continuously release biocidal copper ions has not been investigated.

In this paper, we demonstrate functionalization and recharge of TFC-RO membranes with Cu-NPs to impart antibacterial properties to the membrane surface. The use of a polycation (polyethylenimine) as a capping agent imparts a positive charge to the surface of the Cu-NPs, thereby allowing electrostatic attraction between the NPs and the negatively charged native carboxylic groups on the RO membrane surface. Consequently, binding of the Cu-NPs to the membrane surface requires a simple dip coating procedure, without the need for additional chemical manipulations. This simple functionalization procedure may be repeated to recharge the TFC-membrane surface after Cu-NPs are depleted. The facile functionalization has been shown to impart a strong antibacterial activity to the membrane surface, without degrading the transport properties of the selective polyamide layer, indicating that Cu-NPs are a viable tool for combating TFC-RO membrane biofouling.

MATERIALS AND METHODS

Materials and Chemicals. Copper sulfate ($CuSO_4$), nitric acid (HNO_3), polyethylenimine (PEI) (branched, M_w = 25 000 kDa), and potassium chloride (KCl) were purchased from Sigma Aldrich (St. Louis, MO). Hydrochloric acid (HCl), sodium chloride (NaCl), and 2-propanol (isopropyl alcohol, $CH_3CHOHCH_3$) were received from J.T. Baker (Phillipsburg, NJ). Sodium bicarbonate ($NaHCO_3$) and sodium borohydride ($NaBH_4$) were obtained from Fisher Scientific (Fair Lawn, NJ). Potassium hydroxide (KOH) was purchased from Aventor Performance Materials (Center Valley, PA). Ethanol from Decon Laboratories, Inc. (King of Prussia, PA). Bacto agar and Luria−Bertani (LB) broth were received from BD Biosciences (Sparks, MD) and American Bioanalytical (Natick, MA), respectively. Unless specified, all solutions were prepared in deionized (DI) water (Milli-Q, Millipore, Billerica, MA).

Model Bacteria Strains. Kanamycin resistant *Escherichia coli* (*E. coli*) BW26437 was received from the Yale Coli Genetic Stock Center (New Haven, CT). *Pseudomonas aeruginosa* (*P. aeruginosa*) ATCC 27853 was obtained from the American Type Culture Collection, and *Staphylococcus aureus* (*S. aureus*) 8325 was kindly provided by Dr. Naomi Balaban. Cultures were maintained on LB agar plates and grown in LB media prior to experiments. LB agar plates for *E. coli* included 25 mg/L kanamycin sulfate (American Bioanalytical).

Preparation and Characterization of Copper Nanoparticles (Cu-NPs). A 50 mL Cu-NP suspension was synthesized in the following manner. An aliquot (30 mL) of 0.066 mM PEI solution was added to 10 mL of 50 mM $CuSO_4$ solution and stirred for 5 min at ∼200 rpm. The formation of copper nanoparticles (Cu-NPs) was then initiated by the addition of 10 mL of 100 mM $NaBH_4$, and the suspension was stirred for 25 min at ∼200 rpm. The Cu-NPs were subsequently dialyzed (MWCO of 3500 Da, Spectra/Por dialysis, Spectrum Laboratories, Inc.) for 20 h to remove remaining dissolved salts.

Dynamic light scattering (DLS) (ALV GmbH, Germany) measurements were carried out at an angle of 90°, a wavelength of 532 nm, and 50 cycles (30 s, 10 measurements each).[41] Light absorbance spectra were obtained using UV−vis spectrophotometer (HP 845x). Thermogravimetric analysis (TGA) (TA Instruments, Q500 Thermogravimetric Analyzer) was carried out by first heating 10 mg of the Cu-NP powder for 15 min to 100 °C in a N_2 gas stream (25 mL min^{-1}) to remove moisture and then increasing the temperature to 700 °C at a rate of 10 °C min^{-1}. Before measurement, the Cu-NP sample was freeze-dried to prevent oxidation of the sample during the procedure. A zeta potential analyzer (Zetasizer Nano ZS, Malvern) was used to assess the Cu-NP surface charge. Scanning and transmission electron microscopy were used to characterize the morphology of the Cu-NPs. For SEM, 50 μL of the Cu-NP suspension were placed on a silicon wafer, dried, and sputter-coated (Denton Vacuum, DESK V) with 15 nm chrome prior to analysis (Hitachi ultra-high-resolution analytical field emission scanning electron microscope, FE-SEM, SU-70).

Bright-field transmission electron microscopy (TEM) micrographs of the Cu-NPs were obtained using a FEI Tecnai T12 Spirit Twin TEM/STEM operated at 120 kV and a carbon-coated copper microgrid.

Membrane Functionalization and Characterization. Dried flat sheets of thin-film composite (TFC) polyamide RO membrane (SW30XLE, Dow Filmtec) were received from OctoChem, Inc. The dried membranes were wetted through immersion in 20% isopropanol and 80% DI water for 20 min. The membranes were then rinsed and soaked three times in DI water for 24 h and stored until use at 4 °C.

The TFC membranes were functionalized by dipping in the Cu-NP suspension for 24 h. Before functionalization, the Cu-NP suspension was sonicated (Aquasonic model 150T) for 10 min to disperse Cu-NP aggregates. After the dipping procedure, the membrane was rinsed for ∼10 s with DI water to remove unbound Cu-NPs.

X-ray photoelectron spectroscopy (XPS, Surface Science Instruments model SSX-100− SPECS) measurements were done with monochromatized Al-Kα X-ray source $h\nu$ = 1486.6 eV). Surface hydrophilicity was assessed by surface contact angle measurements with DI water (VCA Video Contact Angle System, AST Products, Billerica, MA). The membrane surface zeta potential was obtained from streaming potential measurements (EKA, Brookhaven Instruments, Holtsville, NY) following the method described previously.[42] Surface roughness was determined using atomic force microscopy (AFM, Bruker Dimension 5000) in tapping mode on 10 different 100 μm^2 spots on three coupons for each membrane sample. Bruker Nano Scope V5.12.5 software was used to calculate the various roughness parameters.

The intrinsic transport properties of the membrane were examined in a standard laboratory-scale RO filtration system.[43] The membrane (area of 20.02 cm^2) was compacted overnight at 31 bar (450 psi), and the pressure was then reduced to 27.6 bar (400 psi) for the measurement of the pure water permeability coefficient, A. Salt rejection was measured with a 50 mM NaCl feed solution at 27.6 bar (400 psi); the salt permeability coefficient, B, was calculated from the measured water flux and salt rejection according to the method described previously.[44] All the filtration experiments were carried out at 25.0 ± 0.5 °C at a cross-flow velocity of 21.4 cm/s.

Cu dissolution from the functionalized membrane was evaluated by placing 3.8 cm^2 coupons of the functionalized membrane in small glass vials. The glass vials were filled with 10 mL of 5 mM $NaHCO_3$ solution (pH 8.25) and agitated. At predetermined time intervals, the solution was removed from the vial for analysis, and 0.1 mL of 70% nitric acid was added to acidify the solution before analysis. The empty glass vial with the membrane was refilled with a DI water (10 mL) and 0.1 mL of 70% nitric acid to dissolve the copper on the membrane that remained after dissolution. The dissolved copper was quantified with an inductive coupled plasma mass-spectrophotometer (ICP-MS, ELAN DRC-e ICP mass spectrometer, Perkin-Elmer).

For measurements of copper loading on the functionalized membrane, a 3.8 cm^2 membrane coupon was placed in 10 mL DI water with 0.1 mL of 70% nitric acid. The dissolved copper ion concentration from the functionalized membrane coupon was quantified by ICP-MS.

Assessing the Antimicrobial Activity of Functionalized Membranes. The antimicrobial properties of the membrane were assessed with three model bacteria: *E. coli, P. aeruginosa*, and *S. aureus*. Bacteria were grown overnight in LB while shaking (190 rpm) at 37 °C. Then, 1 mL of the bacteria grown overnight was diluted in 24 mL fresh LB broth and grown for 2−3 h to exponential phase (determined by a growth curve).

Viable cell attachment experiments were carried out to quantify the number of live bacteria attached to the membrane after 1 h contact time. The prepared bacteria solution was centrifuged (1 min, 5000 rpm, Eppendorf centrifuge 5415D) in 1 mL centrifuge tubes, and then the bacteria were resuspended in an isotonic solution (0.15 M NaCl) with 20 mM $NaHCO_3$ buffer (pH 8.25 ± 0.1) to an optical density at 600 nm (OD_{600}) of 0.25 ± 0.4. A 3.8 cm^2 membrane coupon was placed in the cap of a sterile plastic tube containing the bacteria in solution. When the cap was screwed onto the tube, the active layer alone contacted the bacteria solution. The bacteria were incubated with the membrane for 1 h (37 °C). After incubation, the membranes were rinsed with DI water to remove unattached bacteria. Then, the coupons were sonicated for 7 min in 10 mL of sterile buffered isotonic solution to remove the attached bacteria. The resulting suspension was diluted in the buffered isotonic solution and plated on LB agar plates. After incubation overnight, the number of bacteria colonies on the plates was counted. Plates containing between 3 and 1000 colony-forming units (CFU) were used to calculate the number of bacteria attached to the membrane.

After contact with bacteria, membrane samples were observed with SEM to view changes in cell morphology. The samples were rinsed gently with an isotonic solution, and the bacteria were fixed with 5% glutaraldehyde at −20 °C overnight. The fixed membranes and bacteria were thawed at room temperature and the remaining liquid was removed. Membranes were dried in a desiccator at ambient temperature and coated with 15 nm chrome before SEM imaging.

Statistical Analysis. Significant differences (α = 0.05) were determined using Student's t test (Excel) with two tailed distribution and homoscedastic (two-sample equal variance samples).

RESULTS AND DISCUSSION

Synthesis and Characteristics of Cu-NPs. Very specific characteristics are needed for nanoparticles to be feasible for implementation in RO desalination systems. The nanoparticles must be inexpensive, contain readily available materials, and be produced via a scalable process. The design of Cu-NPs should allow for facile loading onto the membrane surface on site and within the membrane module. In addition, in order to prevent detachment of the Cu-NPs during operation, the Cu-NPs must demonstrate strong affinity for the membrane surface. All these constraints were considered during the design of the Cu-NPs used in this study.

The Cu-NPs were synthesized by a simple wet chemical reduction at ambient conditions. Three main components are involved in this type of synthesis: (1) a precursor metal salt, (2) a capping agent which prevents particle aggregation, and (3) a reducing agent. The capping agent plays a critical role in determining the NP properties. PEI, the chosen Cu-NP capping agent, is relatively inexpensive, readily available, and has been used in numerous applications, including gene delivery[45−47] and water treatment processes.[48−50] A typical branched PEI has high density of amine groups with a theoretical distribution of approximately 25%, 50%, and 25% for primary, secondary, and tertiary amines, respectively.[51] The

protonation of these amine groups imparts a positive electric charge (pK_a 9.5−11[52]) at acidic, neutral, and moderate alkaline pH, thus allowing an electrostatic attraction between the PEI and a negatively charged surface, such as polyamide TFC-RO membranes.

Cu-NP synthesis began with an aqueous $CuSO_4$ solution (light blue, Figure 1A). Addition of PEI to this solution caused

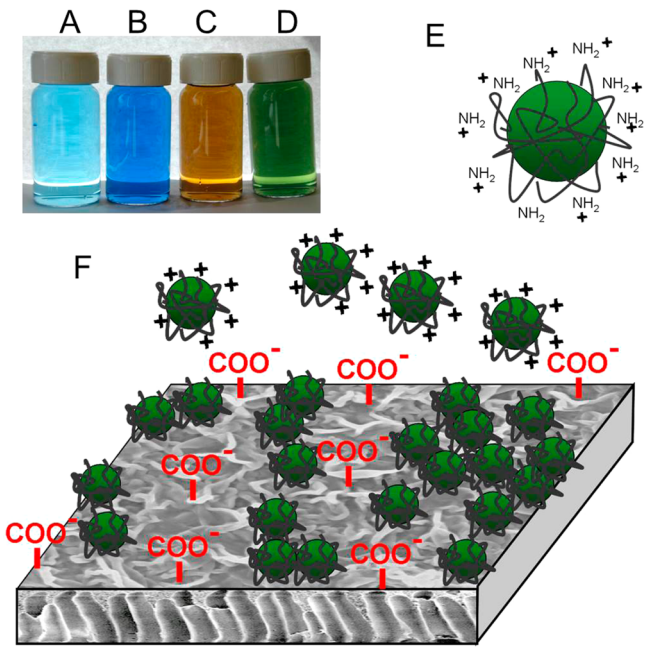

Figure 1. Cu-NP preparation and binding to the TFC membrane active layer. The colors of the Cu-NP suspension at the various synthesis stages are shown for: (A) $CuSO_4$ solution, (B) after addition of PEI and formation of Cu−PEI complexes, (C) after reduction with sodium borohydride, and (D) after 20-h dialysis and oxidation of the Cu-NPs. The amine groups of the PEI impart a positive charge to the Cu-NPs (E). The positively charged Cu-NPs electrostatically bind to the negatively charged native carboxyl groups on the membrane active layer (F).

complexation of PEI amine groups with cupric ions[52] and a subsequent change in solution color from pale blue to dark blue (Figure 1B). Then, addition of $NaBH_4$ led to immediate reduction of cupric ions to form metallic Cu-NPs. Cu-NP formation was accompanied by a change of solution color to brown (Figure 1C). Postsynthesis dialysis was then carried out to purify and remove unreacted species from the Cu-NP suspension. During dialysis, a slow transformation of solution color to green was observed over several hours (Figure 1D).

We surmise that the slow change in suspension color from brown to green during dialysis is attributed to oxidation of metallic Cu-NPs to copper oxide.[53−56] To confirm this assumption, hydrogen peroxide (H_2O_2) was added to a fresh Cu-NP suspension (prior to dialysis) to promote oxidation.[57] The addition of H_2O_2 immediately changed the color of the solution to green. Visual changes in the solution color were confirmed using UV−vis (Figure S1A in Supporting Information (SI)), where the spectra of the dialyzed Cu-NPs strongly resembled that of the fresh Cu-NP suspension treated with H_2O_2. However, it is unknown whether the entire particle or solely the outer layer of the particle was oxidized.[58] In addition, there is uncertainty regarding the speciation of the copper oxide, and it is unknown whether Cu-NPs oxidized to cuprite (Cu_2O),[55,57] tenorite (CuO),[59] or combination of both.[59]

The main objective of this work was to load biocidal copper on the membrane surface through Cu-NP binding. Therefore, it was desired to estimate the copper content in the particles. The last dialysis stage removes unreacted dissolved species from the Cu-NP suspension, specifically $NaBH_4$ and $CuSO_4$. XPS measurements (discussed later) confirmed that the Cu-NPs bound to the membrane surface were composed only of Cu, O, and PEI, without significant content of B, Na, and S (Figure S2 in SI). ICP-MS measurements revealed a high copper production yield, with 90% of the initial copper remaining in the Cu-NP suspension after dialysis. In addition, TGA measurement (Figure 2D) revealed a strong decrease in Cu-

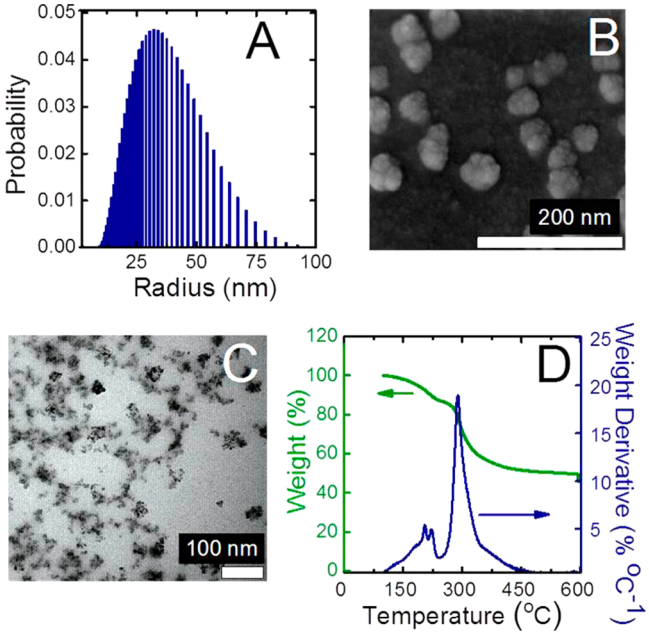

Figure 2. Characteristics of Cu-NP suspension: (A) Cu-NP size (radius) distribution as determined by DLS, B) SEM micrographs of Cu-NPs after drying on a silicon wafer, (C) TEM micrographs of the Cu-NPs, and (D) weight loss and weight derivative (weight loss change) of the Cu-NP suspension during TGA measurements.

NP suspension weight at ∼290 °C, which is related to PEI decomposition and evaporation. Further heating to temperatures above 450 °C did not lead to increment loss of sample mass. Consequently, the remaining 49.5% weight at 450 °C can be related to the inorganic portion of the Cu-NPs, which does not decompose or evaporate. However, not all of the 49.5% inorganic portion is elemental copper, since part of the inorganic fraction is copper oxide. As discussed before, there was uncertainty regarding the dominant copper species present in the oxidized Cu-NPs. Hence, it is estimated that copper makes up between 49.5% (assuming all copper is elemental Cu) and 39% (assuming all of the copper is oxidized to cupric-oxide) of the particle mass.

The Cu-NP suspension was monodispersed with an average radius of 33.8 ± 14.4 nm as obtained from DLS (Figure 2A). SEM images revealed that the Cu-NPs were relatively spherical in shape (Figure 2B). However, TEM micrographs revealed that the particle inner structure does not follow a classic core−shell structure, but each of the 33 nm spherical particles comprises smaller Cu-NPs which aggregated within a matrix of

dx.doi.org/10.1021/es404232s | Environ. Sci. Technol. 2014, 48, 384−393

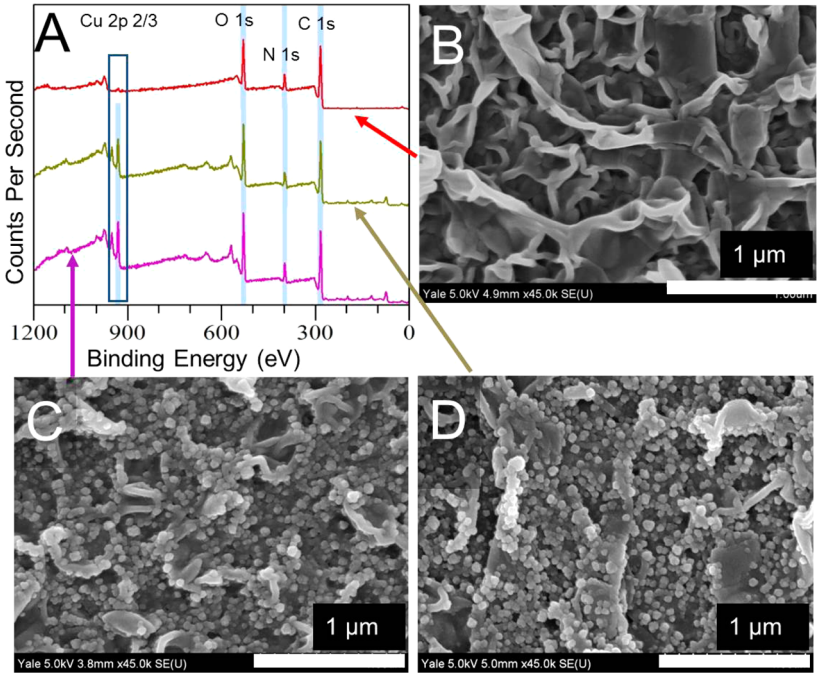

Figure 3. Binding of Cu-NPs to the membrane active layer. A) Counts per second (CPS) vs binding energy (eV) from XPS measurements, with top curve (red) for pristine membrane, middle curve (green) for membrane with bound Cu-NPs after sonication for 5 min, and bottom curve (purple) for membrane with bound Cu-NPs without sonication. SEM micrographs of B) pristine membrane, C) membrane with bound Cu-NPs without sonication, and D) membrane with bound Cu-NPs after sonication of 5 min with DI water.

PEI (Figure 2C). As expected, the Cu-NPs were positively charged (zeta potential of +16.5 mV at pH 8.25) due to protonation of the PEI amine groups. Minimal change in Cu-NP size (less than 5%), as measured by DLS and supported UV−vis spectra, indicated that the produced Cu-NP suspension was stable for at least one week (Figure S1B of SI).

Cu-NPs Strongly Bind to the TFC Membrane. Because the sensitive RO polyamide layer must maintain high salt rejection and water flux in seawater desalination, it is preferable to avoid aggressive chemical modifications to the membrane surface. TFC-RO polyamide membranes have native carboxylic groups on their surface (20−30 nm^{-2}),[60] rendering the surface negatively charged at pH > ∼ 5.[60] We hypothesized that the Cu-NPs with multiple positively charged PEI molecules on their surface (Figure 1E) will have a strong electrostatic attraction with the negatively charged membrane surface. Hence, a facile binding procedure was applied, where the pristine membrane was dip-coated in the Cu-NP suspension, without any chemical manipulation (Figure 1F). Successful binding was confirmed by SEM, revealing an even coating of the membrane surface by Cu-NPs (Figure 3C). Moreover, the Cu-NPs remained bound to the membrane surface after 5 min of sonication in DI water, demonstrating a strong binding of the NPs to the membrane surface (Figure 3D). Electrostatic binding of positively charged NPs on TFC membrane has been shown to remain stable in high salinity solutions and under extreme pH.[11]

Copper loading on the functionalized membrane was confirmed by XPS measurements (Figure 3A). Signal at 932 eV, attributed to Cu 2p 2/3 orbital, appeared in the spectra of the Cu-NP functionalized membrane with and without 5 min sonication and was absent in the spectrum of the pristine membrane. XPS elemental analysis revealed a Cu surface coverage of 3.3 ± 0.7% and 3.0 ± 0.7% for the functionalized and sonicated membranes, respectively (Table S1 in SI).

PEI embedded in the Cu-NPs contains C and N, and due to oxidation, O is expected to be present on the Cu-NPs. However, O, N, and C are also constituents of the RO membrane polyamide layer. This explains the observed signals of these three elements in both the pristine and the functionalized membranes (peaks at 281, 396, and 527 eV for C 1s, N 1s, and O 1s, respectively, in Figure 3A). The small increase in oxygen surface coverage (Table S1 in SI) for the functionalized membranes compared to the pristine membrane, is likely due to the oxidized Cu-NPs. Furthermore, the absence of signals at peaks of 188, 165, and 63 eV, related to boron (B 1s), sulfate (S 2p1/2), and sodium (Na 2s), respectively (Figure S2 in SI), confirmed that these elements, which are introduced during Cu-NP synthesis, were not incorporated into the Cu-NPs and that the Cu-NPs comprised solely copper, copper oxide, and PEI.

The dissolution of Cu-NPs from the functionalized membrane will require reloading after their depletion. Therefore, the same Cu-NP dip-coating functionalization procedure was applied to a membrane that was functionalized and later immersed in DI water for 4 days to dissolve the bound Cu-NPs. The successful reloading of Cu-NPs on the membrane was confirmed by SEM and ICP-MS (Figure S3 in SI). Although it is possible that some residual Cu-NP material remains on the surface, these results indicate that the functionalization did not lead to irreversible changes of the membrane surface chemistry that would prevent repeated reloading of the Cu-NPs on the membrane surface.

Impact of Cu-NP Binding on Membrane Properties. Cu-NP functionalization did not significantly affect the intrinsic membrane transport properties (Figure 4A). After functionalization, the water permeability coefficient of the membrane, *A*,

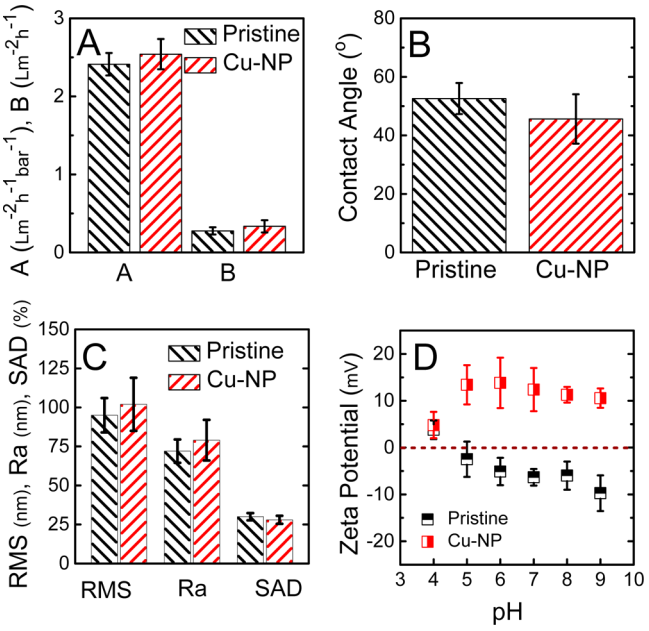

Figure 4. Impact of bound Cu-NPs on membrane properties. (A) Membrane pure water permeability (A) and salt permeability (B) coefficients of pristine and functionalized membranes (n = 4). (B) DI water contact angles of pristine and functionalized membranes (n = 24 on 2 samples). (C) AFM surface morphology parameters of pristine and functionalized membrane: RMS (root-mean-square) in nm, R_a (average roughness) in nm, and SAD (surface area differences) in %. (D) Zeta potential of pristine and functionalized membrane surfaces (n = 6).

did not change significantly: 2.41 ± 0.14 L m^{-2} h^{-1} bar^{-1} for the pristine membrane and 2.54 ± 0.19 L m^{-2} h^{-1} bar^{-1} for the functionalized membrane. Similarly, the salt rejection remained unchanged: 98.86 ± 0.26% for the pristine and 98.6 ± 0.27% for the functionalized membrane. Salt permeability coefficient, B, exhibited only a slight increase after functionalization, from 0.28 ± 0.05 to 0.34 ± 0.05 L m^{-2} h^{-1}, which was statistically insignificant. Since seawater RO has a strict requirement for high salt rejection, the negligible impact on membrane transport properties by the Cu-NP functionalization demonstrates the potential to functionalize less salt selective TFC membranes, such as brackish water RO (BWRO) or nanofiltration (NF).

Membrane propensity for fouling depends on surface physicochemical properties, and a fouling resistant membrane requires that the surface be smooth, hydrophilic, and neutrally charged.[61,62] Cu-NP functionalization did not show a significant impact on membrane hydrophilicity, with measured contact angles of 52.6 ± 5.3° and 45.6 ± 8.4° for the pristine and Cu-NP functionalized membrane, respectively (Figure 4B). Also, functionalization did not significantly impact the membrane surface roughness as determined by AFM (Figure 4C). Root mean square (RMS) roughness increased from 95 ± 11 to 102 ± 17 nm, and other roughness parameters increased only slightly (Figure 4C). The coverage of the membrane with only a monolayer of Cu-NPs explains the minor increase of surface roughness parameters of the functionalized membrane (Figure S4 in Supporting Information).

Membrane surface charge was significantly altered by the Cu-NPs functionalization (Figure 4D). The pristine membrane, with native carboxylic groups, was negatively charged at pH higher than 4, while the functionalized membrane was positively charged at all examined pH values. This positive charge is attributed to the coverage of the membrane surface by the positively charged Cu-NPs. The lower zeta potential of the functionalized membranes at pH 4 may result from rapid dissolution of the Cu-NPs at acidic conditions. At pH 8.25 (pH of the Cu-NP suspension), electrostatic attraction between the negatively charged membrane and the positively charged Cu-NPs (Cu-NP zeta potential of 16.5 mV) predominates.

Antimicrobial Activity of Functionalized Membranes. Functionalization with Cu-NPs significantly reduces the number of viable bacteria attached to the TFC RO membrane (Figure 5). After 1 h contact, the number of attached live

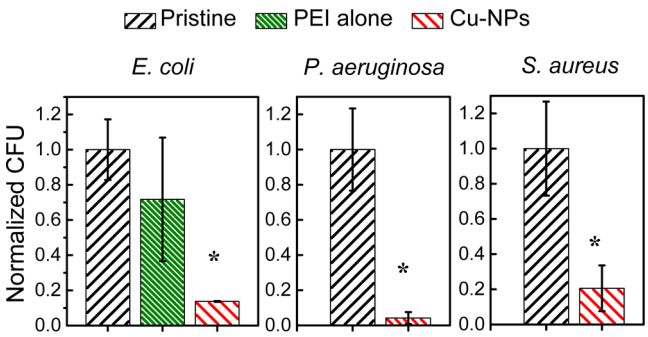

Figure 5. Number of attached live bacteria on pristine (black), PEI alone (green), and Cu-NP (red) membrane for gram negative (*E. coli* and *P. aeruginosa*) and gram positive (*S. aureus*) bacteria. "PEI alone" membrane was contacted overnight with PEI solution (without Cu) at the same PEI concentration (0.04 mM) and same solution pH (8.25) as the Cu-NP solution. The values are normalized to the number of attached live bacteria colonies to the pristine membrane ($N/N_{pristine}$). Experimental conditions: pristine and Cu-NP bound membranes were contacted with bacteria (OD_{600}: 0.25 ± 0.4) in an isotonic solution (0.15 M NaCl; 20 mM $NaHCO_3$ buffer, pH 8.2) for 1 h at 37 °C. After incubation, the membranes were sonicated with sterile isotonic solution and the detached bacteria were plated on LB agar. Asterisks (*) indicate a statistically significant difference between the functionalized and pristine membranes (p < 0.05).

bacteria on the functionalized membrane surface decreased by 87% ± 0.2%, 96% ± 3%, and 79.5% ± 13% for *E. coil, P. aeruginosa,* and *S. aureus*, respectively, relative to the control. These reductions in the number of attached live bacteria on the functionalized membrane were significantly different from the pristine membrane with p-values of less than 0.03 for all three model bacteria. When the same functionalization procedure (the same pH and concentration) was applied with a solution of PEI alone, the reduction in the number of attached live *E. coli* was statistically insignificant (p = 0.41). This observation demonstrates the minor contribution of PEI to the observed reduction in the number of attached live bacteria on the functionalized membrane.

The reduction in the number of attached live bacteria can result from toxicity of the Cu-NPs or a lower attachment rate due to changes in the physicochemical properties of the functionalized membrane surface. As previously discussed, Cu-NP functionalization did not significantly affect membrane surface roughness or hydrophilicity, but the membrane did acquire a positive charge, which likely favors the adhesion of negatively charged bacteria. Therefore, the large reduction in the number of attached live bacteria (80%-95%) on the functionalized membrane is not attributed to a lower deposition rate of bacteria but rather to the toxicity of the bound Cu-NPs.

dx.doi.org/10.1021/es404232s | Environ. Sci. Technol. 2014, 48, 384−393

SEM micrographs of bacteria on the pristine and functionalized membrane (Figure S5 of Supporting Information) showed changes in the cell morphology for bacterial in contact with the Cu-NP functionalized membrane, particularly for *P. aeruginosa* and *E. coli*.

Several previous studies discussed the toxicity of copper to bacteria, algae, fungi, and viruses.[26] The mechanisms of copper toxicity are complex and not fully understood.[63] Past studies suggest that copper increases intracellular reactive oxygen species (ROS) generation, leading to oxidative stress and DNA damage.[64,65] In addition, damage to membrane cell by copper was reported.[66,67] While some studies attributed the toxicity of Cu-NPs solely to leached biocidal copper ions,[65] others suggested additional toxic effects induced by contact with the solid Cu-NPs.[68,69]

Challenges. In order to apply Cu-NPs to RO membrane modules, the Cu-NP functionalization must be rapid and long-lasting. In the current proof-of-concept work, Cu-NP functionalization took several hours, suggesting the need for optimization of our functionalization protocol. As can be seen in Figure 6A, copper loading on the membrane increased with the dip-coating time. In addition, copper loading increases with an increase in Cu-NP concentration in suspension (i.e., lower dilution). After 24 h, a maximum copper loading of 11.99 ± 0.59 $\mu g\ cm^{-2}$ was observed with no dilution. These observations imply that the functionalization rate is mass transfer limited. In the current dipping procedure, the only mass transfer mechanism was diffusion of the Cu-NPs toward the membrane. A possible practical route for increasing the Cu-NP mass transfer is to employ dead-end filtration, which will carry the Cu-NPs toward the membrane via the convective permeate flow. SEM micrographs and ICP-MS measurements demonstrated that large quantities of Cu-NPs can be loaded on the membrane via this method in time scales of only a few minutes (Figure S6 in SI).

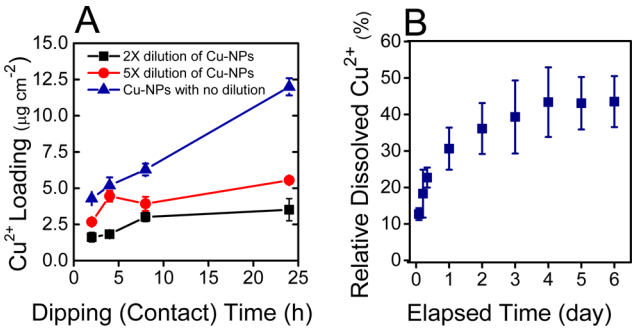

Figure 6. (A) Amount of loaded copper (measured as Cu^{2+}) on the membrane surface for different dipping times (i.e., contact time of pristine membrane in the Cu-NP solution) and for different dilution rates of the Cu-NP suspension. The original Cu-NP suspension was diluted with DI water by 2 or 5 times (indicated in figure) to achieve 50% or 20% of the original Cu-NP concentration, respectively. (B) Cumulative Cu^{2+} dissolved (%) relative to the total copper loaded on the membrane. Dissolution occurred in a 5 mM $NaHCO_3$ solution at pH 8.25 ± 0.1.

For practical application of our method, there is also a need to minimize the frequency of Cu-NP recharge of the membrane surface. This may be realized by loading more copper on the membrane in each recharge event. Higher loading of copper can be achieved by increasing the copper content of the Cu-NPs. Another approach is to increase the number of bound Cu-NPs to achieve higher copper loading (Figure 6A).

However, it appears that the most important factor for lowering the frequency of functionalization is the dissolution rate, which controls the Cu-NP depletion. Consequently, Cu-NP dissolution rate to cupric ions[70] should be optimized. Here, the observed dissolution rate of the Cu-NPs on the functionalized membrane (Figure 6B) was relatively rapid, with dissolution of more than 30% of the loaded copper during the first two days. While the conditions tested here were relatively mild, high ionic strength, acidic pH, chelating agents, or organic ligands may accelerate the Cu-NP dissolution rate.[59,71,72] The hydrodynamic conditions at the membrane surface will also significantly affect the Cu-NPs dissolution rate. Therefore, there is a need to control the Cu-NPs dissolution . One approach to reduce the Cu-NP dissolution rate would be to coat the particles with a relatively insoluble layer. For example, carbon coating of Cu-NPs has been shown to reduce their dissolution rate.[73] However, an extra coating will probably complicate the Cu-NP synthesis, lower the available concentration of Cu^{2+} at the membrane surface, and raise the cost of this modification. In addition, the capping must maintain the positive charge of the NPs for facile and efficient binding by electrostatic attraction to the membrane.

Another challenge is the long-term effect of different types of fouling on both the antibacterial activity of the functionalized membrane and the ability to recharge the Cu-NPs on fouled membrane. The presence of foulants on the membrane may require a precleaning step for each reloading event of the Cu-NPs on the membrane.

Implications. Copper, long known for its antibacterial activity and relatively low cost, is an attractive biocide with a proven history as a biofouling control agent in industrial applications.[74] However, constraints on brine disposal quality and copper implementation costs require precise and efficient use of copper for biofouling control in RO desalination. Localized loading of a copper source in the vicinity of the TFC-RO membrane surface, as demonstrated in the current study, can be an economically attractive method for localized protection of the membrane during the desalination process. The simplicity of the current Cu-NP synthesis and membrane binding, the negligible impact on membrane transport properties, the ability to recharge the Cu-NPs, and the imparted antibacterial activity demonstrate the potential of the suggested method for mitigating biofouling on TFC-RO membranes.

■ ASSOCIATED CONTENT

Supporting Information

UV−vis absorbance of the Cu-NPs suspension under various conditions (Figure S1); XPS spectra of pristine, Cu-NP, and sonicated Cu-NP membranes (Figure S2); SEM micrographs and ICP-MS measurements of copper loading on Cu-NP membranes after functionalization, dissolution, and refunctionalization (Figure S3); SEM micrographs and representative AFM images of pristine and Cu-NP membranes (Figure S4); SEM micrographs of bacteria morphology on pristine and Cu-NP membranes (Figure S5); SEM micrographs and copper loading on Cu-NP membrane functionalized by dead-end filtration (Figure S6); XPS elemental surface coverage of oxygen, carbon, nitrogen, and copper for pristine, Cu-NP, and sonicated Cu-NP membranes (Table S1). This information is available free of charge via the Internet at http://pubs.acs.org/.

AUTHOR INFORMATION

Corresponding Author

*Phone: (203) 432-2789; e-mail: menachem.elimelech@yale.edu.

Notes

The authors declare no competing financial interest.

ACKNOWLEDGMENTS

This publication is based on work supported by Award No. KUS-C1-018-02, granted by King Abdullah University of Science and Technology (KAUST). This research was also supported by BARD, the United States–Israel Binational Agricultural Research and Development Fund, Vaadia-BARD Postdoctoral Fellowship to M.B.-S. (Award No. FI 452-011). This material is also based on work supported by the National Science Foundation Graduate Research fellowship under Grant No. DGE-1122492 awarded to K.R.Z. Any opinion, findings, and conclusions or recommendations expressed in this material are those of the authors and do not necessarily reflect the views of the National Science Foundation.

REFERENCES

(1) Elimelech, M.; Phillip, W. A. The future of seawater desalination: Energy, technology, and the environment. *Science* **2011**, *333* (6043), 712–717.

(2) Baker, J. S.; Dudley, L. Y. Biofouling in membrane systems—A review. *Desalination* **1998**, *118* (1–3), 81–89.

(3) Mansouri, J.; Harrisson, S.; Chen, V. Strategies for controlling biofouling in membrane filtration systems: Challenges and opportunities. *J. Mater. Chem.* **2010**, *20* (22), 4567–4586.

(4) Flemming, H. C.; Schaule, G.; Griebe, T.; Schmitt, J.; Tamachkiarowa, A. Biofouling—The Achilles heel of membrane processes. *Desalination* **1997**, *113* (2–3), 215–225.

(5) Creber, S. A.; Vrouwenvelder, J. S.; van Loosdrecht, M. C. M.; Johns, M. L. Chemical cleaning of biofouling in reverse osmosis membranes evaluated using magnetic resonance imaging. *J. Membr. Sci.* **2010**, *362* (1–2), 202–210.

(6) Glater, J.; Hong, S. K.; Elimelech, M. The search for a chlorine-resistant reverse-osmosis membrane. *Desalination* **1994**, *95* (3), 325–345.

(7) Shemer, H.; Semiat, R. Impact of halogen based disinfectants in seawater on polyamide RO membranes. *Desalination* **2011**, *273* (1), 179–183.

(8) Bernstein, R.; Belfer, S.; Freger, V. Bacterial Attachment to RO membranes surface-modified by concentration-polarization-enhanced graft polymerization. *Environ. Sci. Technol.* **2011**, *45* (14), 5973–5980.

(9) McCloskey, B. D.; Park, H. B.; Ju, H.; Rowe, B. W.; Miller, D. J.; Chun, B. J.; Kin, K.; Freeman, B. D. Influence of polydopamine deposition conditions on pure water flux and foulant adhesion resistance of reverse osmosis, ultrafiltration, and microfiltration membranes. *Polymer* **2010**, *51* (15), 3472–3485.

(10) Sagle, A. C.; Van Wagner, E. M.; Ju, H.; McCloskey, B. D.; Freeman, B. D.; Sharma, M. M. PEG-coated reverse osmosis membranes: Desalination properties and fouling resistance. *J. Membr. Sci.* **2009**, *340* (1–2), 92–108.

(11) Tiraferri, A.; Kang, Y.; Giannelis, E. P.; Elimelech, M. Superhydrophilic thin-film composite forward osmosis membranes for organic fouling control: Fouling behavior and antifouling mechanisms. *Environ. Sci. Technol.* **2012**, *46* (20), 11135–11144.

(12) Kasher R.; Avneri S.; Lutsky M. Y.; Zhang J.; Gellman S. H.; Stahl S. S. Immobilization of antimicrobial polymers on RO membrane to reduce biofilm growth and biofouling. Patent WO2012172547 A1, 2012.

(13) Wei, X. Y.; Wang, Z.; Chen, J.; Wang, J. X.; Wang, S. C. A novel method of surface modification on thin-film-composite reverse osmosis membrane by grafting hydantoin derivative. *J. Membr. Sci.* **2010**, *346* (1), 152–162.

(14) Saeki, D.; Nagao, S.; Sawada, I.; Ohmukai, Y.; Maruyama, T.; Matsuyama, H. Development of antibacterial polyamide reverse osmosis membrane modified with a covalently immobilized enzyme. *J. Membr. Sci.* **2013**, *428*, 403–409.

(15) Tiraferri, A.; Vecitis, C. D.; Elimelech, M. Covalent binding of single-walled carbon nanotubes to polyamide membranes for antimicrobial surface properties. *ACS Appl. Mater. Intefaces* **2011**, *3* (8), 2869–2877.

(16) Miller, D. J.; Araujo, P. A.; Correia, P. B.; Ramsey, M. M.; Kruithof, J. C.; van Loosdrecht, M. C. M.; Freeman, B. D.; Paul, D. R.; Whiteley, M.; Vrouwenvelder, J. S. Short-term adhesion and long-term biofouling testing of polydopamine and poly(ethylene glycol) surface modifications of membranes and feed spacers for biofouling control. *Water Res.* **2012**, *46* (12), 3737–3753.

(17) Mauter, M. S.; Wang, Y.; Okemgbo, K. C.; Osuji, C. O.; Giannelis, E. P.; Elimelech, M. Antifouling ultrafiltration membranes via post-fabrication grafting of biocidal nanomaterials. *ACS Appl. Mater Interfaces* **2011**, *3* (8), 2861–2868.

(18) Banerjee, I.; Pangule, R. C.; Kane, R. S. Antifouling coatings: Recent developments in the design of surfaces that prevent fouling by proteins, bacteria, and marine organisms. *Adv. Mater.* **2011**, *23* (6), 690–718.

(19) Diagne, F.; Malaisamy, R.; Boddie, V.; Holbrook, R. D.; Eribo, B.; Jones, K. L. Polyelectrolyte and silver nanoparticle modification of microfiltration membranes to mitigate organic and bacterial fouling. *Environ. Sci. Technol.* **2012**, *46* (7), 4025–4033.

(20) Sawada, I.; Fachrul, R.; Ito, T.; Ohmukai, Y.; Maruyama, T.; Matsuyama, H. Development of a hydrophilic polymer membrane containing silver nanoparticles with both organic antifouling and antibacterial properties. *J. Membr. Sci.* **2012**, *387*, 1–6.

(21) Zodrow, K.; Brunet, L.; Mahendra, S.; Li, D.; Zhang, A.; Li, Q. L.; Alvarez, P. J. J. Polysulfone ultrafiltration membranes impregnated with silver nanoparticles show improved biofouling resistance and virus removal. *Water Res.* **2009**, *43* (3), 715–723.

(22) Zhang, J. Y.; Zhang, Y. T.; Chen, Y. F.; Du, L.; Zhang, B.; Zhang, H. Q.; Liu, J. D.; Wang, K. J. Preparation and characterization of novel polyethersulfone hybrid ultrafiltration membranes bending with modified halloysite nanotubes loaded with silver nanoparticles. *Ind. Eng. Chem. Res.* **2012**, *51* (7), 3081–3090.

(23) Yang, H. L.; Lin, J. C. T.; Huang, C. Application of nanosilver surface modification to RO membrane and spacer for mitigating biofouling in seawater desalination. *Water Res.* **2009**, *43* (15), 3777–3786.

(24) Yin, J.; Yang, Y.; Hua, H.; Deng, B. Attachment of silver nanoparticles (AgNPs) onto thin-film composite (TFC) membranes through covalent bonding to reduce membrane biofouling. *J. Membr. Sci.* **2013**, *441*, 73–82.

(25) USGS. Metal prices in the United States through 2010. http://pubs.usgs.gov/sir/2012/5188/sir2012-5188.pdf .

(26) Borkow, G.; Gabbay, J. Copper as a biocidal tool. *Curr Med Chem* **2005**, *12* (18), 2163–2175.

(27) Klein, T. Y.; Wehling, J.; Treccani, L.; Rezwan, K. Effective Bacterial inactivation and removal of copper by porous ceramics with high surface area. *Environ. Sci. Technol.* **2013**, *47* (2), 1065–1072.

(28) Albright, L. J.; Wentwort, Jw; Wilson, E. M. Technique for measuring metallic salt effects upon indigenous heterotrophic microflora of a natural water. *Water Res.* **1972**, *6* (12), 1589–1596.

(29) Lin, Y. S. E.; Vidic, R. D.; Stout, J. E.; Yu, V. L. Individual and combined effects of copper and silver ions on inactivation of *Legionella pneumophila*. *Water Res.* **1996**, *30* (8), 1905–1913.

(30) Harrison, J. J.; Ceri, H.; Stremick, C. A.; Turner, R. J. Biofilm susceptibility to metal toxicity. *Environ Microbiol* **2004**, *6* (12), 1220–1227.

(31) Ruparelia, J. P.; Chatteriee, A. K.; Duttagupta, S. P.; Mukherji, S. Strain specificity in antimicrobial activity of silver and copper nanoparticles. *Acta Biomater* **2008**, *4* (3), 707–716.

(32) Environmental Protection Agency, Copper Facts, 2008. http://www.epa.gov/oppsrrd1/REDs/factsheets/copper_red_fs.pdf.
(33) Grass, G.; Rensing, C.; Solioz, M. Metallic copper as an antimicrobial surface. *Appl Environ Microb* **2011**, *77* (5), 1541−1547.
(34) Almeida, E.; Diamantino, T. C.; de Sousa, O. Marine paints: The particular case of antifouling paints. *Prog. Org. Coat.* **2007**, *59* (1), 2−20.
(35) Xu, J.; Feng, X. S.; Chen, P. P.; Gao, C. J. Development of an antibacterial copper (II)-chelated polyacrylonitrile ultrafiltration membrane. *J. Membr. Sci.* **2012**, *413*, 62−69.
(36) Qiu, J. H.; Zhang, Y. W.; Zhang, Y. T.; Zhang, H. Q.; Liu, J. D. Synthesis and antibacterial activity of copper-immobilized membrane comprising grafted poly(4-vinylpyridine) chains. *J. Colloid Interface Sci.* **2011**, *354* (1), 152−159.
(37) Akar, N.; Asar, B.; Dizge, N.; Koyuncu, I. Investigation of characterization and biofouling properties of PES membrane containing selenium and copper nanoparticles. *J. Membr. Sci.* **2013**, *437*, 216−226.
(38) Cornelissen, E. R.; Vrouwenvelder, J. S.; Heijman, S. G. J.; Viallefont, X. D.; Van Der Kooij, D.; Wessels, L. P. Periodic air/water cleaning for control of biofouling in spiral wound membrane elements. *J. Membr. Sci.* **2007**, *287* (1), 94−101.
(39) Araujo, P. A.; Miller, D. J.; Correia, P. B.; van Loosdrecht, M. C. M.; Kruithof, J. C.; Freeman, B. D.; Paul, D. R.; Vrouwenvelder, J. S. Impact of feed spacer and membrane modification by hydrophilic, bactericidal and biocidal coating on biofouling control. *Desalination* **2012**, *295*, 1−10.
(40) Hausman, R.; Gullinkala, T.; Escobar, I. C. Development of copper-charged polypropylene feedspacers for biofouling control. *J. Membr. Sci.* **2010**, *358* (1−2), 114−121.
(41) Pasquini, L. M.; Hashmi, S. M.; Sommer, T. J.; Elimelech, M.; Zimmerman, J. B. Impact of surface functionalization on bacterial cytotoxicity of single-walled carbon nanotubes. *Environ. Sci. Technol.* **2012**, *46* (11), 6297−6305.
(42) Walker, S. L.; Bhattacharjee, S.; Hoek, E. M. V.; Elimelech, M. A novel asymmetric clamping cell for measuring streaming potential of flat surfaces. *Langmuir* **2002**, *18* (6), 2193−2198.
(43) Hoek, E. M. V.; Kim, A. S.; Elimelech, M. Influence of crossflow membrane filter geometry and shear rate on colloidal fouling in reverse osmosis and nanofiltration separations. *Environ. Eng. Sci.* **2002**, *19* (6), 357−372.
(44) Yip, N. Y.; Tiraferri, A.; Phillip, W. A.; Schiffman, J. D.; Elimelech, M. High performance thin-film composite forward osmosis membrane. *Environ. Sci. Technol.* **2010**, *44* (10), 3812−3818.
(45) Lemkine, G. F.; Demeneix, B. A. Polyethylenimines for in vivo gene delivery. *Curr. Opin. Mol. Ther.* **2001**, *3* (2), 178−182.
(46) Kircheis, R.; Kichler, A.; Wallner, G.; Kursa, M.; Ogris, M.; Felzmann, T.; Buchberger, M.; Wagner, E. Coupling of cell-binding ligands to polyethylenimine for targeted gene delivery. *Gene Ther.* **1997**, *4* (5), 409−418.
(47) Forrest, M. L.; Koerber, J. T.; Pack, D. W. A degradable polyethylenimine derivative with low toxicity for highly efficient gene delivery. *Bioconjugate Chem.* **2003**, *14* (5), 934−940.
(48) Vieira, M.; Tavares, C. R.; Bergamasco, R.; Petrus, J. C. C. Application of ultrafiltration-complexation process for metal removal from pulp and paper industry wastewater. *J. Membr. Sci.* **2001**, *194* (2), 273−276.
(49) Molinari, R.; Poerio, T.; Argurio, P. Selective separation of copper(II) and nickel(II) from aqueous media using the complexation-ultrafiltration process. *Chemosphere* **2008**, *70* (3), 341−348.
(50) Geckeler, K. E.; Volchek, K. Removal of hazardous substances from water using ultrafiltration in conjunction with soluble polymers. *Environ. Sci. Technol.* **1996**, *30* (3), 725−734.
(51) Kobayashi, S. Ethylenimine Polymers. *Prog. Polym. Sci.* **1990**, *15* (5), 751−823.
(52) Maketon, W.; Zenner, C. Z.; Ogden, K. L. Removal efficiency and binding mechanisms of copper and copper-EDTA complexes using polyethyleneimine. *Environ. Sci. Technol.* **2008**, *42* (6), 2124−2129.
(53) Jeong, S.; Woo, K.; Kim, D.; Lim, S.; Kim, J. S.; Shin, H.; Xia, Y. N.; Moon, J. Controlling the thickness of the surface oxide layer on Cu nanoparticles for the fabrication of conductive structures by ink-jet printing. *Adv. Funct. Mater.* **2008**, *18* (5), 679−686.
(54) Kanninen, P.; Johans, C.; Merta, J.; Kontturi, K. Influence of ligand structure on the stability and oxidation of copper nanoparticles. *J. Colloid Interface Sci.* **2008**, *318* (1), 88−95.
(55) Chen, C. H.; Yamaguchi, T.; Sugawara, K.; Koga, K. Role of stress in the self-limiting oxidation of copper nanoparticles. *J. Phys. Chem. B* **2005**, *109* (44), 20669−20672.
(56) Tilaki, R. M.; Zad, A. I.; Mahdavi, S. M. Size, composition and optical properties of copper nanoparticles prepared by laser ablation in liquids. *Appl. Phys. A: Mater. Sci. Process.* **2007**, *88* (2), 415−419.
(57) Dhas, N. A.; Raj, C. P.; Gedanken, A. Synthesis, characterization, and properties of metallic copper nanoparticles. *Chem. Mater.* **1998**, *10* (5), 1446−1452.
(58) Son, S. U.; Park, I. K.; Park, J.; Hyeon, T. Synthesis of Cu_2O coated Cu nanoparticles and their successful applications to Ullmann-type amination coupling reactions of aryl chlorides. *Chem. Commun.* **2004**, *7*, 778−779.
(59) Mudunkotuwa, I. A.; Pettibone, J. M.; Grassian, V. H. Environmental implications of nanoparticle aging in the processing and fate of copper-based nanomaterials. *Environ. Sci. Technol.* **2012**, *46* (13), 7001−7010.
(60) Tiraferri, A.; Elimelech, M. Direct quantification of negatively charged functional groups on membrane surfaces. *J. Membr. Sci.* **2012**, *389*, 499−508.
(61) Ostuni, E.; Chapman, R. G.; Holmlin, R. E.; Takayama, S.; Whitesides, G. M. A survey of structure-property relationships of surfaces that resist the adsorption of protein. *Langmuir* **2001**, *17* (18), 5605−5620.
(62) Vrijenhoek, E. M.; Hong, S.; Elimelech, M. Influence of membrane surface properties on initial rate of colloidal fouling of reverse osmosis and nanofiltration membranes. *J. Membr. Sci.* **2001**, *188* (1), 115−128.
(63) Macomber, L.; Rensing, C.; Imlay, J. A. Intracellular copper does not catalyze the formation of oxidative DNA damage in Escherichia coli. *J. Bacteriol.* **2007**, *189* (5), 1616−1626.
(64) Shi, M.; Kwon, H. S.; Peng, Z. M.; Elder, A.; Yang, H. Effects of surface chemistry on the generation of reactive oxygen species by copper nanoparticles. *Acs Nano* **2012**, *6* (3), 2157−2164.
(65) Gunawan, C.; Teoh, W. Y.; Marquis, C. P.; Amal, R. Cytotoxic origin of copper(II) oxide nanoparticles: Comparative studies with micron-sized particles, leachate, and metal salts. *ACS Nano* **2011**, *5* (9), 7214−7225.
(66) Santo, C. E.; Lam, E. W.; Elowsky, C. G.; Quaranta, D.; Domaille, D. W.; Chang, C. J.; Grass, G. Bacterial killing by dry metallic copper surfaces. *Appl. Environ. Microb.* **2011**, *77* (3), 794−802.
(67) Ohsumi, Y.; Kitamoto, K.; Anraku, Y. Changes induced in the permeability barrier of the yeast plasma-membrane by cupric ion. *J. Bacteriol.* **1988**, *170* (6), 2676−2682.
(68) Karlsson, H. L.; Cronholm, P.; Gustafsson, J.; Moller, L. Copper oxide nanoparticles are highly toxic: A comparison between metal oxide nanoparticles and carbon nanotubes. *Chem. Res. Toxicol.* **2008**, *21* (9), 1726−1732.
(69) Midander, K.; Cronholm, P.; Karlsson, H. L.; Elihn, K.; Moller, L.; Leygraf, C.; Wallinder, I. O. Surface characteristics, copper release, and toxicity of nano- and micrometer-sized copper and copper(II) oxide particles: A cross-disciplinary study. *Small* **2009**, *5* (3), 389−399.
(70) Pacioni, N. L.; Filippenko, V.; Presseau, N.; Scaiano, J. C. Oxidation of copper nanoparticles in water: Mechanistic insights revealed by oxygen uptake and spectroscopic methods. *Dalton Trans.* **2013**, *42*, 5832−5838.
(71) Levard, C.; Mitra, S.; Yang, T.; Jew, A. D.; Badireddy, A. R.; V., L. G.; B., G. E., Jr. Effect of chloride on the dissolution rate of silver nanoparticles and toxicity to *E. Coli*. *Environ. Sci. Technol.* **2013**, *47* (11), 5738−5745.

(72) Wang, Z.; Bussche, A. V. D.; Kabadi, P. K.; Kane, A. B.; Hurt, R. H. Biological and environmental transportations of copper-based nanomaterials. *ACS Nano* **2013**, *7* (10), 8715−8727.
(73) Studer, A. M.; Limbach, L. K.; Van Duc, L.; Krumeich, F.; Athanassiou, E. K.; Gerber, L. C.; Moch, H.; Stark, W. J. Nanoparticle cytotoxicity depends on intracellular solubility: Comparison of stabilized copper metal and degradable copper oxide nanoparticles. *Toxicol. Lett.* **2010**, *197* (3), 169−174.
(74) Saeed, M. O.; Jamaluddin, A. T.; Tisan, I. A.; Lawrence, D. A.; Al-Amri, M. M.; Chida, K. Biofouling in a seawater reverse osmosis plant on the Red Sea coast, Saudi Arabia. *Desalination* **2000**, *128* (2), 177−190.